JOC Article

Bonded Exciplexes. A New Concept in Photochemical Reactions

Yingsheng Wang, Olesya Haze, Joseph P. Dinnocenzo,* and Samir Farid*

Department of Chemistry, University of Rochester, Rochester, New York 14627

Ramy S. Farid*

Schrödinger, Inc., 120 West 45th Street, 29th Floor, New York, New York 10036

Ian R. Gould*

Department of Chemistry and Biochemistry, Arizona State University, Tempe, Arizona 85287

igould@asu.edu

Received May 31, 2007

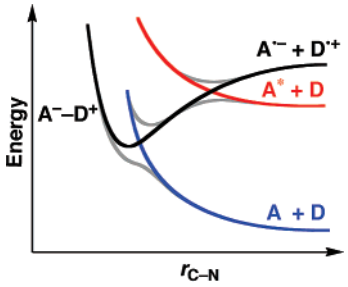

Charge-transfer quenching of the singlet excited states of cyanoaromatic electron acceptors by pyridine is characterized by a driving force dependence that resembles those of conventional electron-transfer reactions, except that a plot of the log of the quenching rate constants versus the free energy of electron transfer is displaced toward the endothermic region by 0.5−0.8 eV. Specifically, the reactions with pyridine display rapid quenching when conventional electron transfer is highly endothermic. As an example, the rate constant for quenching of the excited dicyanoanthracene is 3.5×10^9 M^{-1} s^{-1}, even though formation of a conventional radical ion pair, $A^{\bullet-}D^{\bullet+}$, is endothermic by ∼0.6 eV. No long-lived radical ions or exciplex intermediates can be detected on the picosecond to microsecond time scale. Instead, the reactions are proposed to proceed via formation of a previously undescribed, short-lived charge-transfer intermediate we call a "bonded exciplex", A^-—D^+. The bonded exciplex can be formally thought of as resulting from bond formation between the unpaired electrons of the radical ions $A^{\bullet-}$ and $D^{\bullet+}$. The covalent bonding interaction significantly lowers the energy of the charge-transfer state. As a result of this interaction, the energy decreases with decreasing separation distance, and near van der Waals contact, the A^-—D^+ bonded state mixes with the repulsive excited state of the acceptor, allowing efficient reaction to form A^-—D^+ even when formation of a radical ion pair $A^{\bullet-}D^{\bullet+}$ is thermodynamically forbidden. Evidence for the bonded exciplex intermediate comes from studies of steric and Coulombic effects on the quenching rate constants and from extensive DFT computations that clearly show a curve crossing between the ground state and the low-energy bonded exciplex state.

1. Introduction

In the conventional model for charge-transfer quenching of excited states, the product is described in terms of single electron transfer from a donor (D) to an acceptor (A), which for neutral reactants generates a geminate radical ion pair ($A^{\bullet-}D^{\bullet+}$).[1] In a bimolecular reaction, the radical ions in the initially formed pair may be in contact or separated by solvent.[1,2] The more general term exciplex (Ex) describes the product of a photoinduced electron-transfer reaction in which the extent of charge transfer can be variable.[3] Variable charge transfer in an exciplex is

(1) (a) Weller, A. *Z. Phys. Chem. (Munich)* **1982**, *130*, 129. (b) Mataga, N. *Pure Appl. Chem.* **1984**, *9*, 1255. (c) Gould, I. R.; Farid, S. *Acc. Chem. Res.* **1996**, *29*, 522.

10.1021/jo071157d CCC: $37.00
Published on Web 08/04/2007

explained by mixing between the pure radical ion pair state ($A^{\bullet-}D^{\bullet+}$), the pure locally excited state (A*D) in the case of an excited acceptor, and the neutral ground state (AD), eq 1.[3] The larger the coefficient c_1 in eq 1, the more the exciplex resembles a pure contact radical ion pair ($A^{\bullet-}D^{\bullet+}$), which is thus a limiting

$$\Psi(\mathrm{Ex}) = c_1\Psi(A^{\bullet-}D^{\bullet+}) + c_2\Psi(A^*D) + c_3\Psi(AD) \quad (1)$$

case of the more general exciplex.[4] The magnitude of c_1 is determined mainly by the relative energies of the ($A^{\bullet-}D^{\bullet+}$) and (A*D) states; the contribution from AD, c_3, is usually very small. For cyanoanthracene acceptors and alkylbenzene donors, the exciplexes have largely radical ion pair character (~95%) when the energies of ($A^{\bullet-}D^{\bullet+}$) are lower than those of (A*D) by ca. 0.2 eV.[4] The conventional radical ion pair/exciplex model forms the basis of the well-known Rehm−Weller description of photoinduced electron-transfer kinetics[5] and can also provide a quantitative description of the electronic properties of exciplexes.[4]

Considering the enormous amount of work that is based on the conventional radical ion pair model, any exceptions would clearly be of interest. We have found such an exception in the charge-transfer quenching of cyanoaromatics by pyridine. Quenching of 9,10-dicyanoanthracene (DCA) fluorescence by pyridine has previously been described in a series of papers by Jacques and co-workers, who noted a general increase in the efficiency of quenching by pyridine and related *n*-donors compared to corresponding π-donors such as substituted benzenes.[6] These reactivity differences were attributed to unusually high Coulombic stabilization of the *n*-donor radical ion pairs.[6a,c] We have now further investigated this and related reactions in detail and have found that the Coulombic argument is insufficient to explain the reaction kinetics. Indeed, the results cannot be explained in terms of the conventional electron-transfer model at all. Specifically, pyridine quenches the fluorescence of DCA with a rate constant that approaches the diffusion-controlled limit even though formation of a radical ion pair in this case is endothermic by more than ~0.6 eV! Here we propose a *new mechanism for charge-transfer quenching* that is based on *covalent bond formation* between organic reactants and show

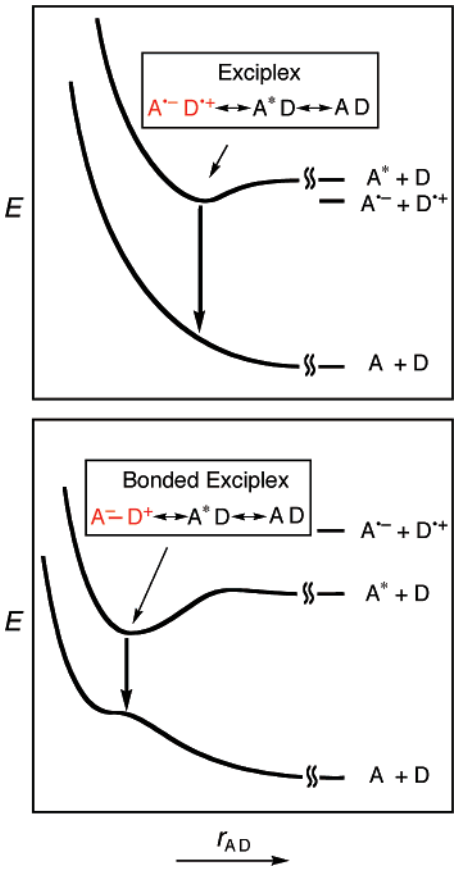

FIGURE 1. Schematic illustration of the energies of (top) a conventional exciplex and (bottom) a bonded exciplex, as a function of separation distance. The bottom panel shows that as the separation distance approaches van der Waals contact the covalent bonding interaction can result in a product that is much lower in energy than that of the locally excited state (A* + D), even when the energy of the nonbonded radical ions ($A^{\bullet-}$ + $D^{\bullet+}$) is much higher than the locally excited state.

how the conventional model (eq 1) needs to be modified to properly describe these reactions.

In the conventional model, the unpaired electrons are localized on the individual radical ions. However, if the electrons can spin pair to form a covalent bond, then a *bonded* charge-transfer state (A^-−D^+) would result. The wavefunction to describe this "bonded exciplex" is given by eq 2, which differs from eq 1 by substitution of ($A^{\bullet-}D^{\bullet+}$) with (A^-−D^+). A bonded exciplex shares a number of similarities with a conventional exciplex.

$$\Psi(\mathrm{Ex}) = c_1'\Psi(A^-{-}D^+) + c_2\Psi(A^*D) + c_3\Psi(AD) \quad (2)$$

Both have charge-transfer character and, in both, the ground-state interaction between the donor and acceptor is repulsive at the geometry of the excited state. Both exciplexes can also decay to the ground state to regenerate the starting materials, and importantly, both can potentially lead to new stable organic products. The most important difference is that with decreasing separation distance the covalent bonding interaction leading to the bonded exciplex can significantly lower the energy of the charge-transfer state compared to the nonbonded radical ion pair state, Figure 1. In turn, this can allow a quenching reaction that would otherwise be energetically forbidden. In addition to representing a new intermediate, the most important feature of the bonded exciplex structure is obviously formation of a new

(2) (a) Gould, I. R.; Young, R. H.; Farid, S. *J. Phys. Chem.* **1991**, *95*, 2068. (b) Arnold, B. R.; Noukakis, D.; Farid, S.; Goodman, J. L.; Gould, I. R. *J. Am. Chem. Soc.* **1995**, *117*, 4399. (c) Peters, K. S. In *Advances in Electron Transfer Chemistry*; Mariano, P. S., Ed.; Jai Press: Greenwich, CT, 1994; Vol. 4, p 27.

(3) (a) Murrell, J. N. *J. Am. Chem. Soc.* **1959**, *81*, 5037. (b) Mulliken, R. S.; Person, W. B. *Molecular Complexes: A Lecture and Reprint Volume*; Wiley-Interscience: New York, 1969. (c) Beens, H.; Weller, A. In *Organic Molecular Photophysics*; Birks, J. B., Ed.; Wiley: New York 1975; Vol. 2, Chapter 4. (d) Mataga, N. In *The Exciplex*; Gordon, M., Ware, W. R., Eds.; Academic: New York, 1975. (e) Bixon, M.; Jortner, J.; Verhoeven, J. W. *J. Am. Chem. Soc.* **1994**, *116*, 7349.

(4) (a) Gould, I. R.; Young, R. H.; Mueller, L. J.; Albrecht, A. C.; Farid, S. *J. Am. Chem. Soc.* **1994**, *116*, 8188. (b) Gould, I. R.; Young, R. H.; Mueller, L. J.; Albrecht, A. C.; Farid, S. *J. Am. Chem. Soc.* **1994**, *116*, 3147.

(5) Rehm, D.; Weller, A. *Isr. J. Chem.* **1970**, *8*, 259.

(6) (a) Jacques, P.; Haselbach, E.; Henseler, A.; Pilloud, D.; Suppan, P. *J. Chem. Soc., Faraday Trans.* **1991**, *87*, 3811. (b) Jacques, P.; Burget, D. *J. Photochem. Photobiol. A: Chem.* **1992**, *68*, 165. (c) Ghoneim, N.; Hammer, C.; Haselbach, E.; Pilloud, D.; Suppan, P.; Jacques, P. *J. Chem. Soc., Faraday Trans.* **1993**, *89*, 4271. (d) Jacques, P.; Allonas, X. *J. Chem. Soc., Faraday Trans.* **1993**, *89*, 4267. (e) Jacques, P.; Allonas, X. *J. Photochem. Photobiol. A: Chem.* **1994**, *78*, 1. (f) Jacques, P.; Burget, D. *New J. Chem.* **1995**, *19*, 1061. (g) Jacques, P.; Allonas, X. *Chem. Phys. Lett.* **1995**, *233*, 533. (h) Jacques, P.; Burget. D.; Allonas, X. *New J. Chem.* **1996**, *20*, 933.

covalent bond. A wide range of bond-forming organic reactions have been discovered that are initiated by photoinduced single electron transfer.[7] Bonded exciplexes may represent important previously unidentified intermediates in many of these reactions.

As we will show, the quenching reactions of excited aromatic electron acceptors with pyridines and related donors can best be understood if their products are bonded exciplexes (Figure 1). The bonded exciplex model properly accounts for the excited-state quenching and radiationless decay behavior of the quenching products. The model is supported by combined experimental and DFT computational studies that clearly show a curve crossing between the ground state and the low-energy bonded exciplex state, manifested by a deviation from purely repulsive behavior on the ground-state surface, Figure 1.

This paper is divided into several parts. The first describes photophysical studies on the reactions of a variety of excited-state acceptors with pyridines and related donors. The second introduces a curve-crossing model involving a bonded exciplex that accounts for all of the important experimental observations. The third describes quantum mechanical calculations that support the curve-crossing model. The fourth describes an example of charge-transfer quenching via *both* bonded and nonbonded exciplexes. Finally, we discuss the potential generality of this mechanism beyond the scope of the reactions presented in this paper.

2. Results and Discussion

2.1. Experimental Photophysical Observations. The ^{1}DCA*/Pyridine Reaction. DCA has been widely used in electron transfer photochemical and photophysical studies.[8] Its relatively long-lived singlet excited state (11−15 ns), high fluorescence quantum yield in many solvents (>0.9), and well-characterized radical anion make it a convenient acceptor/sensitizer for the study of many reactions.[8] The absorption spectra of DCA in neat pyridine, acetonitrile, and cyclohexane give no indication of any ground-state interactions with pyridine. The DCA fluorescence is considerably quenched in the presence of pyridine (see further below); however, the residual emission is very similar to that in the absence of pyridine, and no additional bands can be observed. Steady-state irradiation (at 405 nm) of DCA in acetonitrile in the presence of 0.8 M pyridine was performed to look for consumption of DCA. No change in the UV−vis absorption spectrum of DCA was detected after extended irradiation. Using chemical actinometry,[9] the quantum yield for DCA consumption was determined to be ≪1%, even when ∼99% of the DCA fluorescence was quenched. Thus, the reaction of ^{1}DCA* with pyridine results exclusively in the regeneration of the starting materials.

Transient Absorption Spectroscopy. Transient absorption experiments were carried out in different solvents in an attempt to identify potential reaction intermediates. If single electron transfer was involved, then separated radical ions may be formed.[8a] However, when DCA was excited in acetonitrile in the presence of 0.5 M pyridine, no absorption due to DCA$^{\bullet-}$ at 705 nm[8a] could be detected on the nanosecond to microsecond time scale. Attempts to trap pyridine radical cations using dimethoxystilbene, which enhances the sensitivity of radical cation detection due to the large extinction coefficient of its own radical cation,[8a] also failed to yield any detectable signal.

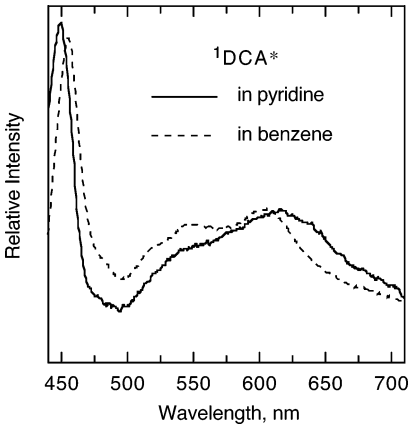

FIGURE 2. Transient spectrum of excited DCA (355 nm, 20 ps) in pyridine and in benzene.

Shown in Figure 2 is the transient absorption spectrum measured 30 ps after excitation of DCA in neat pyridine, using a 355 nm, 20 ps excitation pulse, together with the corresponding spectrum in benzene. The spectrum in both cases is assigned to ^{1}DCA*. The spectrum in pyridine decays rapidly, consistent with efficient quenching, whereas it is long-lived in benzene, where the emission of ^{1}DCA* is not quenched at all. Apart from some small wavelength shifts and a slight broadening in pyridine the absorption spectrum of ^{1}DCA* is similar in both solvents, although both are also broader than the corresponding spectrum in acetonitrile (the spectra in the other solvents are provided in the Supporting Information). The spectra in toluene and 2,6-lutidine are somewhat sharper than in pyridine or benzene, even though the former compounds are better electron donors. The spectrum in the sterically hindered 2,6-di-*tert*-butylpyridine is as sharp as that observed in acetonitrile. These observations suggest that the spectrum of ^{1}DCA* in pyridine is unremarkable and is slightly broadened due to a specific solvent interaction in aromatic solvents, such as benzene, rather than due to any charge-transfer interaction.

The time dependence of the ^{1}DCA* absorption signal in pyridine at both 450 and 640 nm was measured after excitation using a 390 nm, 120 fs laser pulse (Figure 3). A major decay component was observed at both wavelengths with the same time constant, 1.7×10^{10} s^{-1} ($\tau \sim 60$ ps). A faster component with a time constant of 1.3×10^{11} s^{-1} was also observed as growth at 450 nm and a decay at 650 nm, which is presumably due to a fast ($\tau \sim 8$ ps) solvent relaxation.[10] As mentioned above, the emission spectrum of ^{1}DCA* in neat pyridine can be measured and, although weak, exhibits the same shape and

(7) See, for example: (a) Mattes, S.; Farid, S. In *Organic Photochemistry*; Padwa, A., Ed.; Dekker: New York, 1983; Vol. 6, p 233. (b) Lewis, F. D. In *Photoinduced Electron Transfer, Part C*; Fox, M. A., Chanon, M., Eds.; Elsevier: Amsterdam, 1988; p 1.

(8) See, for example: (a) Gould, I. R.; Ege, D.; Moser, J. E.; Farid, S. *J. Am. Chem. Soc.* **1990**, *112*, 4290. (b) Ware, W. R.; Holmes, J. D.; Arnold, D. R. *J. Am. Chem. Soc.* **1974**, *96*, 7861. (c) Evans, T. R.; Wake, R. W.; Jaenicke, O. In *The Exciplex*; Gordon, M., Ware, W. R., Eds.; Academic Press: New York, 1975; p 345. (d) Farid, S.; Brown, K. A. *J. Chem. Soc., Chem. Commun.* **1976**, *14*, 564. (e) Eriksen, J.; Foote, C. S.; Parker, T. L. *J. Am. Chem. Soc.* **1977**, *99*, 6455. (f) Schaap, A. P.; Zaklika, K. A.; Bashir, K.; Fung, L. W. M. *J. Am. Chem. Soc.* **1980**, *102*, 389. (g) Ohashi, M.; Kudo, H.; Yamada, S. *J. Am. Chem. Soc.* **1979**, *101*, 2201.

(9) Brown-Wensley, K. A.; Mattes, S. L.; Farid, S. *J. Am. Chem. Soc.* **1978**, *100*, 4162.

(10) (a) Johnson, A. E.; Levinger, N. E.; Kliner, D. A. V.; Tominaga, K.; Barbara, P. F. *Pure Appl. Chem.* **1992**, *64*, 1219. (b) Zeglinski, D. M.; Waldeck, D. H. *J. Phys. Chem.* **1988**, *92*, 692. (c) Maroncelli, M. *J. Mol. Liq.* **1993**, *57*, 1. (d) Fleming, G. R.; Cho, M. *Annu. Rev. Phys. Chem.* **1996**, *47*, 109. (e) Chang, Y. J.; Simon, J. D. *Springer Ser. Phys. Chem.* **1996**, *62*, 253. (f) Cramer, C. J.; Truhlar, D. G. *Chem. Rev.* **1999**, *99*, 2161.

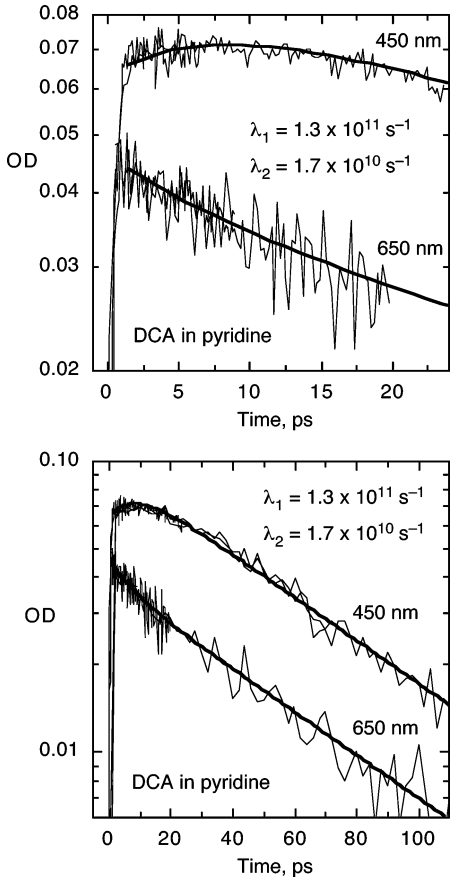

FIGURE 3. Semilogarithmic plot of the absorption decay of excited DCA (390 nm, 120 fs) in pyridine monitored at 450 and 650 nm. The data were collected over several different time scales and then combined. The top figure is an expansion of the lower figure at early times.

vibronic structure as in other solvents. A quantitative comparison of the emission intensity of ^{1}DCA* fluorescence in neat pyridine and in neat 2,6-lutidine was performed. Lutidine was chosen because the ^{1}DCA* emission is quite strong in this solvent due to relatively slow reaction (see further below), but its refractive index is similar to pyridine, and the ^{1}DCA* radiative rate constant is presumably similar in both solvents. An emission lifetime of 4.8 ns is easily measured in lutidine. The ratio of the emission quantum yields is ~1.5:100 for pyridine/lutidine, which gives a predicted lifetime for ^{1}DCA* in neat pyridine of ca. 70 ps. This agrees reasonably well with the transient absorption decay lifetime of ca. 60 ps and provides further support to the assignment of the spectrum in Figure 2 to ^{1}DCA* and not, for example, to an exciplex intermediate.

Transient absorption spectra for ^{1}DCA* in neat pyridine and also in benzene and acetonitrile in the presence of high concentrations of pyridine were recorded as a function of time (these spectra are included in the Supporting Information). At all time delays the spectra were identical to that of ^{1}DCA*, and no spectral changes were observed that might indicate formation of other intermediates.

These combined experiments clearly indicate that the only detectable transient intermediate formed by excitation of DCA in the presence of pyridine is ^{1}DCA*. Other reactive intermediates either cannot be observed under our conditions or their decay rates must be significantly faster ($>10^{10}$ s^{-1}) than their rates of formation.

Rate Constants for Quenching by Pyridine. In conventional photoinduced electron-transfer reactions, the rate constants for electron transfer usually correlate with the driving force ($-\Delta G$). For reactions of an excited acceptor in a polar solvent, where Coulombic stabilization can be neglected, the driving force is given by eq 3.[1a,5] Here, E_{A^*} and E^{red}_A are the excited-state energy and reduction potential of the acceptor, and E^{ox}_D is the oxidation potential of the donor.

$$-\Delta G = E_{A^*} - (E^{ox}_D - E^{red}_A) \qquad (3)$$

For reactions in which the driving force exceeds ~0.2 eV, the values of the rate constants plateau at the diffusion-controlled limit.[5] As the driving force decreases, so does the rate constant for electron transfer, and when the electron transfer becomes endothermic by ~0.3 eV, electron transfer becomes too slow to compete with the decay of the singlet excited states of most organic molecules ($\tau \sim 10$ ns).[5]

The rate constant for the reaction of ^{1}DCA* with pyridine was compared to those of other excited cyanoaromatic acceptors to determine the dependence of the quenching rate constants on the driving force for electron transfer. Stern−Volmer constants (K_{SV}) for quenching of several excited cyanoanthracene and cyanonaphthalene derivatives by pyridine in acetonitrile were obtained from plots of the ratio of fluorescence intensity in the absence and in the presence of pyridine (Φ_0/Φ) versus pyridine concentration. K_{SV} is equal to the product of the quenching rate constant and the lifetime of the excited acceptor, $k_q\tau_{A^*}$. The rate constant data are summarized in Table 1 and are plotted as a function of the free energy change for the reactions, ΔG, in Figure 4. ΔG is simply the negative of the driving force and is calculated with eq 3 using an oxidation potential for pyridine (E^{ox}_D) of 2.62 V versus SCE (see below) and parameters for the sensitizers given in Table 1. Qualitatively, the shape of the plot is similar to that expected for electron-transfer reactions, being close to diffusion controlled when exothermic and decreasing in the endothermic region. However, for the pyridine reactions, the rate constants do not start to decrease until the reaction is endothermic by ca. 0.5 eV, which is clearly inconsistent with the usual radical ion pair mechanism for electron-transfer reactions.

The quenching reactions of excited cyanoaromatics with alkylbenzenes as donors have previously been studied extensively, and these reactions have been shown to proceed via single electron transfer with formation of radical ion pair intermediates.[2,4,8a,11] The rate constants for these reactions were measured to compare with the pyridine reactions (see the Supporting Information) and are also included in Figure 4.[12] The dependence on reaction free energy for these reactions is as expected for the radical ion pair model; the rate is diffusion controlled when sufficiently exothermic and decreases rapidly

(11) (a) Gould, I. R.; Young, R. H.; Farid, S. In *Photochemical Processes in Organized Molecular Systems*; Honda, K., Ed.; Elsevier: Amsterdam, 1991. (b) Gould, I. R.; Mueller, J. L.; Farid, S. *Z. Phys. Chem. (Munich)* **1991**, *170*, 143. (c) Gould, I. R.; Farid, S.; Young, R. H. *J. Photochem. Photobiol. A: Chem.* **1992**, *65*, 133. (d) Gould, I. R.; Farid, S. *J. Phys. Chem.* **1992**, *96*, 7635. (e) Gould, I. R.; Noukakis, D.; Gomez-Jahn, L.; Young, R. H.; Goodman, J. L.; Farid, S. *Chem. Phys.* **1993**, *176*, 439. (f) Arnold, B. R.; Noukakis, D.; Farid, S.; Goodman, J. L.; Gould, I. R. *J. Am. Chem. Soc.* **1995**, *117*, 4399. (g) Gould, I. R.; Moser, J. E.; Armitage, B.; Farid, S. *Res. Chem. Intermediates* **1995**, *21*, 793. (h) Gould, I. R.; Boiani, J. A.; Gailard, E. B.; Goodman, J. L.; Farid, S *J. Phys. Chem. A* **2003**, *107*, 3515.

TABLE 1. Cyanoaromatic Acceptors, Their Excitation Energies (E_{A^*}), Reduction Potentials (E^{red}_A), Singlet Excited-State Lifetimes (τ_{A^*}), and Quenching Rate Constants by Pyridine, k_q (Py), and 2,6-Lutidine, k_q (Lut), in Argon-Purged Acetonitrile

acceptor		E_{A^*}[a] (eV)	E^{red}_A[a] (V vs SCE),	τ_{A^*} (ns)	k_q (Py) (10^9 M^{-1} s^{-1})	k_q (Lut) (10^9 M^{-1} s^{-1})
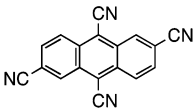	TCA	2.87	-0.44	16.8	9.8	10.7
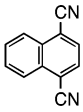	DCN	3.57	-1.27	10.3	11.0	5.6
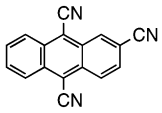	TriCA	2.85	-0.67	18.0	8.0	1.5
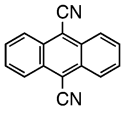	DCA	2.90	-0.91	14.9	3.5[b]	0.089
	1CN	3.83	-1.88	8.9	2.0	0.036
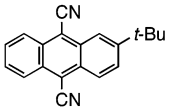	tB-DCA	2.84	-0.95	16.3	2.0	–[c]
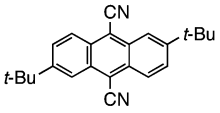	DtB-DCA	2.80	-0.99	17.0	0.84	–[c]
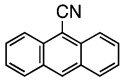	9CA	3.03	-1.45	17.0	0.025	–[c]

[a] Used to calculate the reaction driving force, eq 3, together with oxidation potentials for pyridine and lutidine of 2.62 and 2.37 V versus SCE, respectively; see text. [b] The corresponding quenching rate constant in cyclohexane is 1.8×10^9 M^{-1} s^{-1}. [c] The quenching rate constant is too small to measure.

as the driving force becomes endothermic. A good fit to the alkylbenzene data can be obtained using the Rehm−Weller equation with a reorganization energy of 1.5 kcal/mol.[5] The cyanoaromatic/pyridine data cannot be fitted to the Rehm−Weller equation, and an interpolated line is drawn through these data points.

It is instructive to compare the reactions of ^{1}DCA* with pyridine ($k_q = 3.5 \times 10^9$ M^{-1} s^{-1}) and with benzene, where the quenching is below the detection limit ($k_q < 5 \times 10^6$ M^{-1} s^{-1}). The rate constant for the pyridine reaction is ca. 3 orders of magnitude larger than the benzene reaction despite the fact that both reactions have essentially the same driving force for formation of a radical ion pair (see below). The more efficient

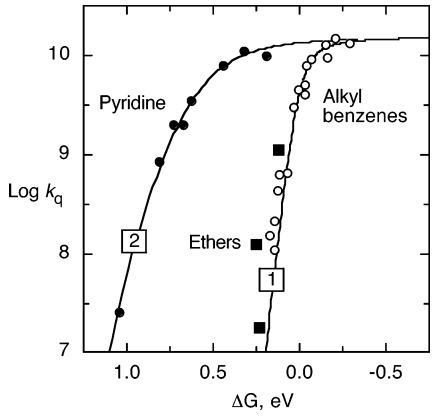

FIGURE 4. Logarithm of the rate constants for quenching of singlet excited cyanoaromatic acceptors by alkylbenzene donors (1, open circles) and by pyridine (2, filled circles) in acetonitrile. The pyridine data are from Table 1, and the benzene data are provided in the Supporting Information. The filled squares are data for quenching of excited cyanoaromatic acceptors by dioxane and 1,2-dimethoxyethane as donors (see text).

(12) (a) With the exception of toluene, the oxidation potentials for the alkylbenzenes used to calculated the reaction exothermicities were taken from ref 8a. The oxidation potential of toluene was estimated to be 2.33 V versus SCE based on measurements in trifluoroacetic acid.[12b,c] In trifluoroacetic acid, the reported oxidation potentials of the other alkylbenzenes, when referenced versus SCE, are on average ~0.02 V higher than those in ref 8a. (b) Howell, J. 0.; Goncalves, J. M.; Amatore. C.; Klasinc, L.; Wightman, R. M.; Kochi, J. K. *J. Am. Chem. Soc.* **1984**, *106*, 3968. (c) Amatore. C.; Lefrou, C. *J. Electroanal. Chem.* **1992**, *325*, 239.

TABLE 2. Pyrylium Salts, Their Excitation Energies (E_{A^*}), Reduction Potentials (E^{red}_A), Singlet Excited-State Lifetimes (τ_{A^*}), and Rate Constants (k_q) for Quenching of Their Excited States by Pyridine in Argon-Purged Acetonitrile

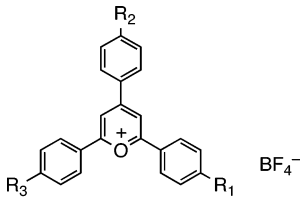

P

pyrylium acceptor	R_1	R_2	R_3	E_{A^*} (eV)	E^{red}_A (V vs SCE)	τ_{A^*} (ns)	k_q (10^9 M^{-1} s^{-1})
P1	H	H	H	2.83	−0.32	4.38	8.7
P2	Et	H	Et	2.67	−0.38	4.96	2.3
P3	Me	Me	Me	2.70	−0.42	∼4.6	∼2.2
P4	CN	H	CN	2.90	−0.11	3.80	16.0
P5	H	CN	H	2.73	−0.19	5.43	11.0
P6	Et	CN	Et	2.58	−0.25	5.85	3.6
P7	OEt	H	H	2.44	−0.40	1.75	0.33
P8	OEt	H	OEt	2.40	−0.46	2.25	∼0.05

quenching by pyridine has been previously attributed to greater Coulombic stabilization of radical ion pair intermediates for *n*-donors.[6a,c]

To test this hypothesis, we studied reactions with positively charged excited-state acceptors that generate radical cation/neutral radical pairs that lack Coulombic stabilization. *N*-Methylacridinium (NMA^+) was initially selected because its excited-state properties (E_{A^*} = 2.80 eV, E^{red} = −0.46 V vs SCE, τ_{A^*} = 34 ns) closely resemble those of 2,6,9,10-tetracyanoanthracene (TCA), one of the cyanoaromatics in Figure 4, in all important respects except for its charge.[13] The quenching rate constant for reaction of $^1NMA^{+}$* with pyridine (7.3×10^9 M^{-1} s^{-1}) was found to be similar to that for ^{1}TCA* (Table 1), providing initial evidence against the Coulombic hypothesis. Because of the difficulty of obtaining acridinium salts with varying reduction potentials, additional experiments were performed using a series of pyrylium salts.[14] The pyrylium salt kinetic data are summarized in Table 2 and illustrated in Figure 5. For comparison, the corresponding quenching rate constants with alkylbenzenes as donors were also measured (Figure 5, data provided in the Supporting Information). The quenching rate constants for reaction of the alkylbenzenes with the excited cyanoaromatics and with the excited pyrylium salts were found to be virtually indistinguishable (open triangles and line 1 in Figure 5). In contrast, the reactions of the excited pyrylium cations with pyridine are again considerably faster, with the rate constants decreasing only when the reactions are endothermic by at least 0.25 eV. These data show that the difference in the quenching behavior for the pyridine and the alkylbenzene donors cannot be due solely to enhanced Coulombic stabilization; an alternate explanation is required. Unlike with the alkylbenzene donors, the cyanoaromatic and pyrylium salt quenching curves with pyridine are somewhat displaced.

(13) (a) The negatively charged counterion may contribute to stabilization in less polar solvents than acetonitrile where ion pairing may be significant.[13b] (b) Todd, W. P.; Dinnocenzo, J. P.; Farid, S.; Goodman, J. L.; Gould, I. R., *J. Am. Chem. Soc.* **1991**, *113*, 3601.

(14) The rate constants for quenching of some excited pyrylium salts were also reported by Jacques et al.[6d]

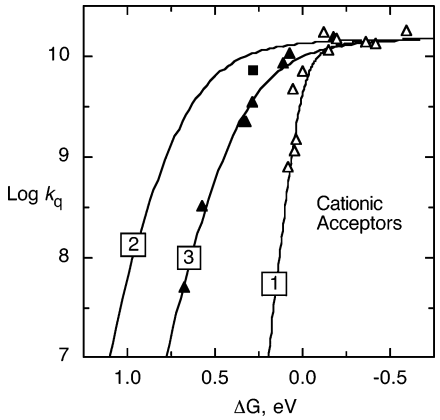

FIGURE 5. Logarithm of the rate constants for quenching of singlet excited pyrylium acceptors by alkylbenzene donors (line 1, open triangles) and pyridine (line 3, filled triangles) in acetonitrile. The data are from Table 2 and the Supporting Information. The curve through the alkylbenzene data (1) is the same as that drawn through the cyanoaromatic data of Figure 4. The curve labeled (2) is the same as that drawn through the pyridine data of Figure 4. The filled square is the point for reaction of excited *N*-methylacridinium with pyridine. The curve labeled (3) is drawn by simple interpolation through the pyrylium data points.

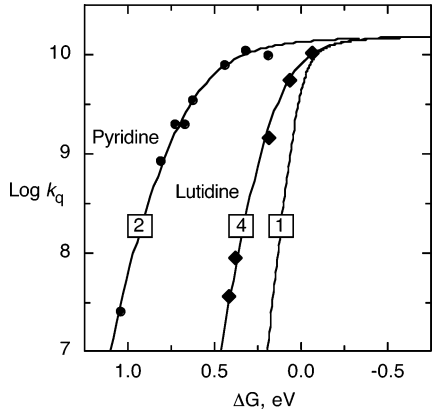

FIGURE 6. Logarithm of the rate constants for quenching of singlet excited cyanoanthracene acceptors by 2,6-lutidine (4, filled diamonds) and pyridine (2, filled circles, from Figure 4). The curve labeled (1) represents the best fit to the data for alkylbenzenes as donors from Figure 4.

The reason for this difference will be discussed below in the context of the quenching mechanism.

Rate Constant for Reaction with 2,6-Lutidine. Previous work by Jacques and co-workers has shown that substituents on the pyridine ring, particularly those in the ortho positions to nitrogen, can significantly influence the excited-state quenching reactions of pyridines.[6b] We have measured quenching rate constants for reaction of various excited cyanoaromatics with 2,6-lutidine (Table 1 and Figure 6). Our results confirm the previously reported steric effect;[6b] most of the lutidine reactions are substantially slower than those with pyridine. An additional feature of the kinetic data for lutidine is discussed in more detail below (section 2.4).

Rate Constants for Reaction of Ethers. To further test the proposal that radical ion pairs generated from *n*-donors like pyridine might enjoy unusually large Coulombic stabilization, we also investigated the quenching of excited-state cyanoaromatics with a different class of *n*-donors, dialkyl ethers. The

rate constants for quenching of ^{1}TCA* and ^{1}DCN* by dioxane were found to be 1.1×10^9 and 1.3×10^8 M^{-1} s^{-1}, respectively. The rate constant for quenching of ^{1}TCA* by dimethoxyethane was 1.8×10^7 M^{-1} s^{-1}. These data are included in Figure 4. These rate constants clearly lie very close to those of the alkylbenzene reactions, which are known to proceed by conventional electron transfer. The ether quenching data are inconsistent with an unusual Coulombic stabilization of radical ion pairs for *n*-donors. The results also reveal a fundamental difference between the quenching mechanisms for the ether donors and pyridine.

Oxidation Potentials of Pyridines and Ethers. The key observation from the pyridine quenching reactions described above is that, with both cyanoaromatic and pyrylium sensitizers, the rate constants are too large to be explained by formation of geminate, radical cation/radical anion or radical cation/radical pairs. This conclusion rests on the estimated thermodynamics for the electron-transfer reactions, which requires the oxidation potentials of pyridine, lutidine, and the ethers *in acetonitrile*. Unfortunately, no reliable electrochemical measurements have been reported for these molecules, and determination of these potentials is decidedly nontrivial. Here we describe in detail the methods we have used to determine these oxidation potentials. We initially attempted time-resolved radical cation equilibration experiments;[15] however, these were unsuccessful due to the very short lifetimes of the pyridine radical cations. Therefore, other methods were pursued. We first describe determination of the oxidation potential of 2,6-lutidine from exciplex emission spectra.

Exciplex emission spectra *in acetonitrile* can be readily measured for ^{1}1CN* and ^{1}DCN* as acceptors with several alkylbenzenes as donors, Figure 7.[16] The average emission frequencies of the reduced spectra depend upon the reduction potential of the acceptor, the oxidation potential of the donor, and the reorganization energy.[11e] The bandwidths of these spectra are very similar, which implies similar reorganization energies.[17] Accordingly, a plot of the average emission frequency[11e] versus $E^{ox}_D - E^{red}_A$ is linear with a slope of *unity*, Figure 8. The corresponding exciplex spectrum for DCN with lutidine as the donor can also be readily measured, Figure 7. The bandwidth of this spectrum is similar to those of the alkylbenzene exciplexes, which indicates that the reorganization energy is also similar. Thus, the oxidation potential for 2,6-lutidine can be obtained by comparison of its average emission frequency with those of the alkylbenzenes, whose oxidation potentials in acetonitrile are known.[12] As illustrated in Figure 8, this allows a determination of the oxidation potential for 2,6-lutidine of 2.37 V versus SCE. The fact that the difference between the ionization potential and the estimated oxidation potential for 2,6-lutidine is equal to that for toluene and is only slightly larger than that for *m*-xylene (Table 3) requires similar

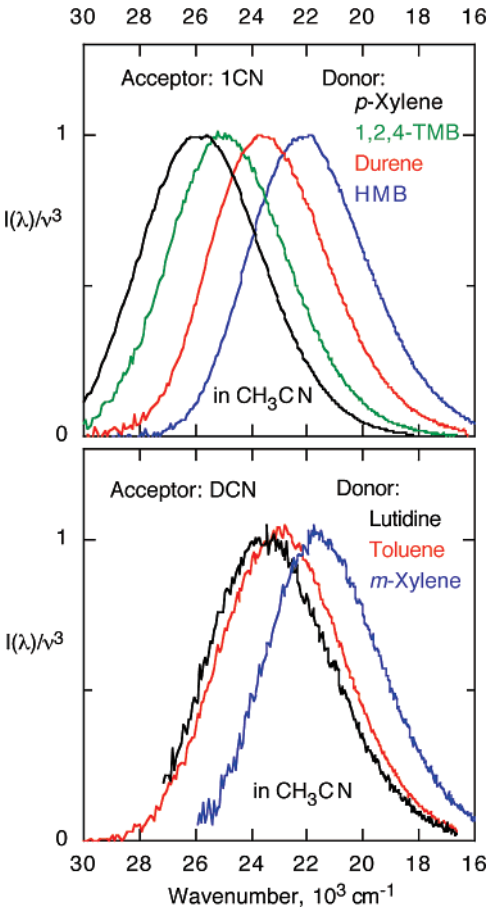

FIGURE 7. Reduced emission spectra of 1-cyanonaphthalene (top) and 1,4-dicyanonaphthalene exciplexes with alkylbenzenes and with 2,6-lutidine in acetonitrile.

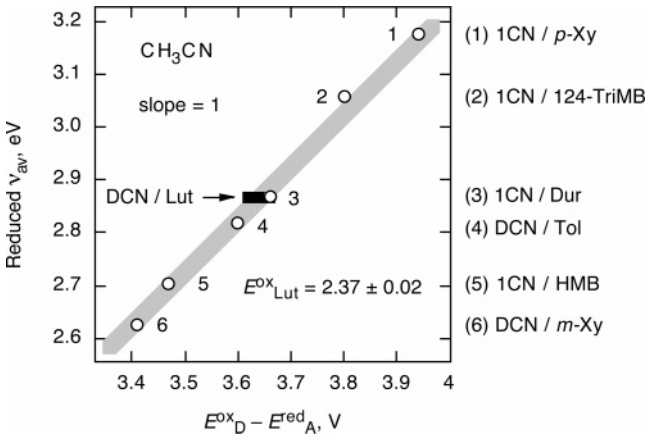

FIGURE 8. Plot of average emission frequency of the reduced exciplex spectra from Figure 7 versus the difference in oxidation potential of the donor and reduction potential of the acceptor. The exciplexes are those of alkylbenzenes with 1-cyanonaphthalene (1CN) and 1,4-dicyanonaphthalene (DCN). The line is drawn with a slope of unity. The average emission frequency for the DCN/lutidine exciplex is indicated by the filled rectangle, from which a value for the lutidine oxidation potential of 2.37 ± 0.02 V versus SCE is obtained by interpolation.

(15) Guirado, G.; Fleming, C. N.; Lingenfelter, T. G.; Williams, M. L.; Zuilhof, H.; Dinnocenzo, J. P. *J. Am. Chem. Soc.* **2004**, *126*, 14086.

(16) Exciplex emission spectra in acetonitrile have now been reported for a number of systems; see, for example, refs 4a, 11d, and: (a) Gould, I. R.; Young, R. H.; Mueller, L. J.; Farid, S. *J. Am. Chem. Soc.* **1994**, *116*, 8176. (b) Gould, I. R.; Farid, S. *J. Am. Chem. Soc.* **1993**, *115*, 4814. (c) Olea, A. F.; Worrall, D. R.; Wilkinson, F. *Photochem. Photobiol. Sci.* **2003**, *2*, 212. (d) Sadovskii, A.; Kutsenok, O. I.; Vainshtein, Y. A.; Kuzmin, M. G. *Zh. Fiz. Khim.* **1996**, *70*, 2194. (e) Mac, M.; Kwiatkowski, P.; Turek, A. M. *Chem. Phys. Lett.* **1996**, *250*, 104. (f) Kikuchi, K *Chem. Phys. Lett.* **1990**, *173*, 421.

(17) For more detailed discussions of the analysis of the bandwidths of such exciplex spectra, the derivation of reduced spectra from measured spectra, and the determination of ion pair energies from such spectra, see ref 11e. The similarity in the reorganization energies for these systems contrasts with that found for corresponding emissions of the smaller electron acceptor tetracyanobenzene with various alkylbenzene donors, where a decrease in reorganization energy with increasing substitution (and thus size) of the donor could be detected.[11e]

TABLE 3. Ionization Potentials (IP) and Oxidation Potentials (E^{ox}) for Various Donors and Their Differences

compound	IP[a]	E^{ox} (V vs SCE)[b]	IP−E^{ox}
m-xylene	8.55	2.14	6.41
2,6-lutidine	8.86	2.37	6.49
toluene	8.82	2.33	6.49
benzene	9.24	2.60	6.64
pyridine	9.26	*2.62*[c]	*6.64*[d]

[a] Data from ref 18. [b] The oxidation potentials are obtained as described in the text and ref 12. [c] Value estimated by assuming that IP − E^{ox} is the same as that for benzene (see text). [d] Assumed to be the same as that for benzene (see text).

solvation energies for the radical cations of similarly substituted benzenes and pyridines. Assuming that this trend holds for benzene and pyridine, we can estimate an oxidation potential for pyridine from the corresponding oxidation potential for benzene.

Unfortunately, corresponding exciplex spectra cannot be observed using benzene or pyridine because the oxidation potential of benzene is too high to quench ^{1}CN* and ^{1}DCN*, and pyridine quenches by formation of a bonded exciplex (see below). Furthermore, no accurate electrochemical oxidation potential can be measured for benzene in acetonitrile. However, an estimate for the benzene oxidation potential can be obtained from a known correlation between oxidation potential and ionization potential. Kochi et al. have reported that a plot of oxidation potential for alkylbenzenes in trifluoroacetic acid versus ionization potential is linear.[12b,c] The slope was found to be less than unity, which was attributed to increased solvent stabilization of the radical cation (which decreases the oxidation potential) with decreasing number of methyl substituents on the benzene ring.[12b,c] Such a plot using oxidation potentials for the alkylbenzenes included in the current study from ref 12a versus recent ionization potentials from ref 18 yields $E^{ox} = 0.735 \times (IP - 4.137)$ (see the Supporting Information). Extrapolation of this plot to the ionization potential for benzene (9.24 eV) yields a value of ∼2.65 V versus SCE for the oxidation potential in acetonitrile. The benzene oxidation potential can also be estimated from the cyanoaromatic and pyrylium salt fluorescence quenching experiments described above (Figures 4 and 5). For benzene to fit with the Rehm−Weller descriptions of the quenching data shown in these figures, an oxidation potential of 2.60 V versus SCE is required. This is very close to the value obtained from the ionization potential plot. Thus, we conclude that the best estimate for the oxidation potential of benzene in acetonitrile is 2.60 V versus SCE. The ionization potential for pyridine (9.26 eV)[18] is very close to that of benzene (9.24 eV).[18] If we assume the same difference in oxidation potentials, this leads to an oxidation potential of ∼2.62 V versus SCE for pyridine (Table 3). This oxidation potential was used to generate the data in Figures 3−5.

A potential problem with the above analysis is that the lowest ionization potential of the benzenes and also of 2,6-lutidine correspond to removal of a π electron, whereas the lowest ionization potential of pyridine reaction corresponds to removal of an electron from a nonbonding orbital.[19] It is important to consider the possibility that, due to its more localized nature, the pyridine radical cation might have increased solvent stabilization relative to a π-delocalized radical cation. This would mean that the difference in oxidation and ionization potentials might be larger for pyridine compared to benzene. There are two arguments against this concern. First, if the efficient quenching of cyanoaromatic excited states by pyridine were due to a conventional electron-transfer reaction with formation of a highly solvated *n*-pyridine radical cation, then the rate constant should be dramatically lower in nonpolar solvents. However, the quenching rate constant of ^{1}DCA* by pyridine in cyclohexane is smaller than in acetonitrile by only a factor of 2 (1.8×10^9 vs 3.5×10^9 M^{-1} s^{-1}), which can be accounted for by the ratio of the viscosities of the two solvents. This lack of dependence on solvent polarity argues against exceptional solvation of *n*-radical cations and also against electron transfer to form a radical ion pair intermediate. Second, the quenching data for the dialkyl ethers shown in Figure 4 argue against large solvent stabilization of *n*-electron donors in general.

The ionization potentials of dioxane (9.19 eV) and 1,2-dimethoxyethane (9.30 eV) are similar to that of benzene (9.24 eV).[18] If we assume a similar relationship between the ionization and oxidation potentials for these ethers and benzene, oxidation potentials of 2.55 and 2.66 V versus SCE are estimated for dioxane and 1,2-dimethoxyethane, respectively. Using these oxidation potentials, the quenching rate constants for the ethers fit closely with those of alkyl benzenes (Figure 4), indicating there is no exceptional solvent stabilization of the ether radical cations versus the alkyl benzene radical cations. Finally, we note that the ionization potential of pyridine (9.26 eV) is intermediate between that of dioxane (9.19 eV) and 1,2-dimethoxyethane (9.30). Therefore, one would have expected pyridine to be of intermediate reactivity *if* it reacted with the excited-state sensitizers by conventional electron transfer, as the ethers do. However, pyridine is orders of magnitude more reactive than the ethers, strongly suggesting that it reacts by another mechanism.

2.2. The Bonded Exciplex Model. Perhaps the most mechanistically revealing observation is the strong rate retardation for excited-state quenching by pyridine when substituted at the C2 and C6 positions (lutidine), which is clearly attributable to a steric effect. The observation suggests a quenching process involving bonding between the pyridine and the excited-state sensitizers. As discussed in the Introduction, a possible model to explain the quenching process for pyridines is that, unlike conventional exciplex formation, the reactions with pyridines involve mixing of the locally excited (LE) configuration with a *bonded*, electron-transfer (ET) configuration.

Figure 9 shows a configuration mixing diagram, of the type pioneered by Shaik,[20] that illustrates the relative energies of the ground, locally excited (LE), and electron-transfer (ET) configurations as a function of decreasing separation distance (r_{C-N}) during formation of a bonded exciplex between excited-state

(18) Lias, S. G.; Bartmess, J. E.; Liebman, J. F.; Holmes, J. L.; Levin, R. D.; Mallard, W. G. "Ion Energetics Data" in *NIST Chemistry WebBook, NIST Standard Reference Database Number 69*; Linstrom, P. J., Mallard, W. G., Eds.; June 2005, National Institute of Standards and Technology, Gaithersburg MD, 20899 (http://webbook.nist.gov).

(19) For a literature summary regarding the assignment of the lowest ionic state of pyridine, see: Tsubouchi, M.; Suzuki, T. *J. Phys. Chem. A* **2003**, *107*, 10897.

(20) (a) Shaik, S. S. *J. Am. Chem. Soc.* **1981**, *103*, 3692. (b) Pross, A.; Shaik, S. S. *Acc. Chem. Res.* **1983**, *16*, 363. (c) Shaik, S. S. *Prog. Phys. Org. Chem.* **1985**, *15*, 197. (d) Shaik, S. S. In *New Theoretical Concepts for Understanding Organic Reactions*; Bertrán, J., Csizmadia, I. G., Eds.; NATO ASI Series; Kluwer: Dordrecht, The Netherlands, 1989; Vol. C267, p 165. (e) Shaik, S.; Shurki, A. *Angew. Chem., Int. Ed.* **1999**, *38*, 586.

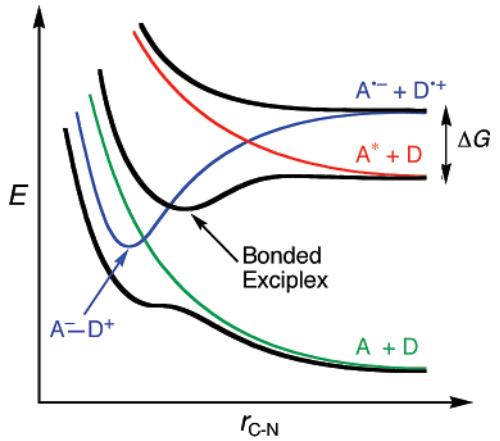

FIGURE 9. Schematic representation of energies for ground, locally excited, and electron-transfer configurations versus distance between the nitrogen atom of pyridine (D) and a carbon atom of the acceptor (A). The repulsive ground configuration (A + D) is represented by the green curve and the locally excited configuration of the acceptor (A* + D) by the red curve. The Morse-shaped (blue) curve represents the bonded electron-transfer configuration ($A^{-}-D^{+}$), which gives $A^{\bullet-}$ and $D^{\bullet+}$ at the dissociation limit. The heavy, black curves represent the mixed states; the bottom of the middle curve is the bonded exciplex. Note that, whereas conventional electron transfer is strongly endothermic (positive ΔG), bond formation lowers substantially the electron-transfer state, which allows for strong coupling with the excited state.

electron acceptors and pyridine.[21] At large separation distances, the energy of the (blue) ET configuration ($A^{\bullet-} + D^{\bullet+}$) lies well above the LE configuration. As r_{C-N} decreases, the energy of the ET configuration drops due to C−N bond formation and eventually crosses the (red) LE configuration. As a consequence, the LE and ET configurations mix, which results in a smaller activation energy for quenching relative to that required to form a nonbonded $A^{\bullet-} + D^{\bullet+}$ state. In this respect, the bonded exciplex model fundamentally differs from that for conventional exciplexes, where the energies of both the LE and ET configurations rise with decreasing A/D separation distance. Figure 9 also shows that at short distances the bonding interaction can be sufficiently stabilizing that the bonded ET configuration can cross the (green) repulsive ground electronic configuration. The mixing in this second, curve-crossing region results in an excited state with a small energy gap to the ground state. Significantly, this latter crossing also results in a ground-state energy profile that deviates from the purely repulsive behavior expected in the absence of low-energy $A^{-}-D^{+}$ configuration.

The "bonded exciplex" model qualitatively explains all of the important experimental observations regarding the quenching of excited states by pyridines. For example, it rationalizes the steric effects observed for pyridines substituted at the C2/C6 positions because the crossing region of the LE and ET configurations almost certainly occurs at a smaller separation distance than van der Waals contact where steric effects will become important. Strong mixing between the LE and ET configurations at the crossing point also lowers the activation barrier for quenching by pyridine, consistent with rapid reaction even when single electron transfer is highly endothermic. Furthermore, the model predicts that as A* becomes a better electron acceptor the energy of the ET configuration will decrease, leading to a further lowering of the barrier height for quenching, as observed. Next we present computational evidence for the bonded exciplex model.

2.3. DFT Computational Studies. The three-configuration mixing scheme of Figure 9 was tested computationally by exploring the energy surface for interaction of pyridine with *ground-state* acceptors. Density functional theory (DFT) calculations were used to evaluate the energy profile for interaction of pyridine with acceptors as a function of the distance between the pyridine nitrogen and one of the carbon atoms of the acceptor (r_{C-N}). For computations of energy surfaces in the vicinity of curve crossings, a multi-configurational method such as CASSCF is often employed.[22] However, one of us has recently shown that, for a related problem involving mixed radical states as a function of σ-bond stretching, CASSCF and the more economical density functional theory gave similar results.[21e] Therefore, all computations were performed with the B3LYP hybrid-functional method. In addition, the self-consistent reaction field (SCRF) implicit solvation model in Jaguar[23] (which utilizes a Poisson−Boltzmann solver) was used to simulate the solvent, acetonitrile. All calculations were corrected for basis set superposition error with the counterpoise method,[24] and geometries were fully optimized at each r_{C-N} distance.

The results of the computations are shown in Figure 10 for seven of the reactions studied experimentally. The calculated energies show an initial rise as the r_{C-N} distance decreases beyond van der Waals contact. Importantly, as r_{C-N} decreases, the energy surfaces exhibit clear inflection points near ∼2 and ∼1.6 Å. These "kinks" in the energy surfaces indicate a crossing, or near crossing, of electronic configurations, as illustrated in Figure 9. One of the contributors must be the ground configuration represented by the acceptor and pyridine. The other is presumably the bonded ET configuration. This assignment is supported by the calculations, as described below.

Most of the computations in Figure 10 were performed using a 6-31G** basis set. The 6-31G** basis set was compared to the 6-31+G** set for addition of pyridine to DCA at the C2 position, as shown in Figure 10A. The use of diffuse functions results in somewhat lower energies. This is expected because the diffuse functions presumably account better for the electron correlation that surely is important for mixed systems such as these.[25] The general shape of the energy surfaces is essentially the same for both basis sets, however. Thus, we conclude that the 6-31G** set provides a good *qualitative* description of the surfaces, but that 6-31+G** is required for a more quantitative description.

(21) For leading references to the use of similar curve-crossing models, see: (a) Michl, J. *Phys. Chem.* **1975**, *7*, 125. (b) Saveant, J.-M. *Adv. Electron Transfer Chem.* **1994**, *4*, 53. For some references to recent applications of similar models, see: (c) Burghardt, I.; Laage, D.; Hynes, James, T. *J. Phys. Chem. A* **2003**, *107*, 11292. (d) Lorance, E. D.; Gould, I. R. *J. Phys. Chem. A* **2005**, *109*, 2912. (e) Lorance, E. D.; Hendrickson, K.; Gould, I. R. *J. Org. Chem.* **2005**, *70*, 2014−2020.

(22) See, for example: (a) Matsunaga, N.; Yarkony, D. R. *J. Chem. Phys.* **1997**, *107*, 7825. (b) Bearpark, M. J.; Robb, M. A.; Yamamoto, N. *Spectrochim. Acta Part A* **1999**, *55*, 639. (c) Blancafort, L.; Adam, W.; Gonzalez, D.; Olivucci, M.; Vreven, T.; Robb, M. A. *J. Am. Chem. Soc.* **1999**, *121*, 10583. (d) Diau, E. W.-G.; De Feyter, S.; Zewail, A. H. *Chem. Phys. Lett.* **1999**, *304*, 134. (e) Robb, M. A.; Olivucci, M. *J. Photochem. Photobiol. A* **2001**, *144*, 237. (f) Quenneville, J.; Ben-Nun, M.; Martínez, T. J. *J. Photochem. Photobiol. A* **2001**, *144*, 229. (g) Klessinger, M. *J. Photochem. Photobiol. A* **2001**, *144*, 217. (h) Blancafort, L.; Jolibois, F.; Olivucci, M.; Robb, M. A. *J. Am. Chem. Soc.* **2001**, *123*, 722.

(23) *Jaguar*, version 6.5 (build 112); Schrödinger Inc.: Portland, OR.

(24) Ratner, M. A.; Schatz, G. C. *Introduction to Quantum Mechanics in Chemistry*; Prentice Hall: Upper Saddle River, NJ, 2001; p 230

(25) Jensen, F. *Introduction to Computational Chemistry*; Wiley: New York, 1999; p 156.

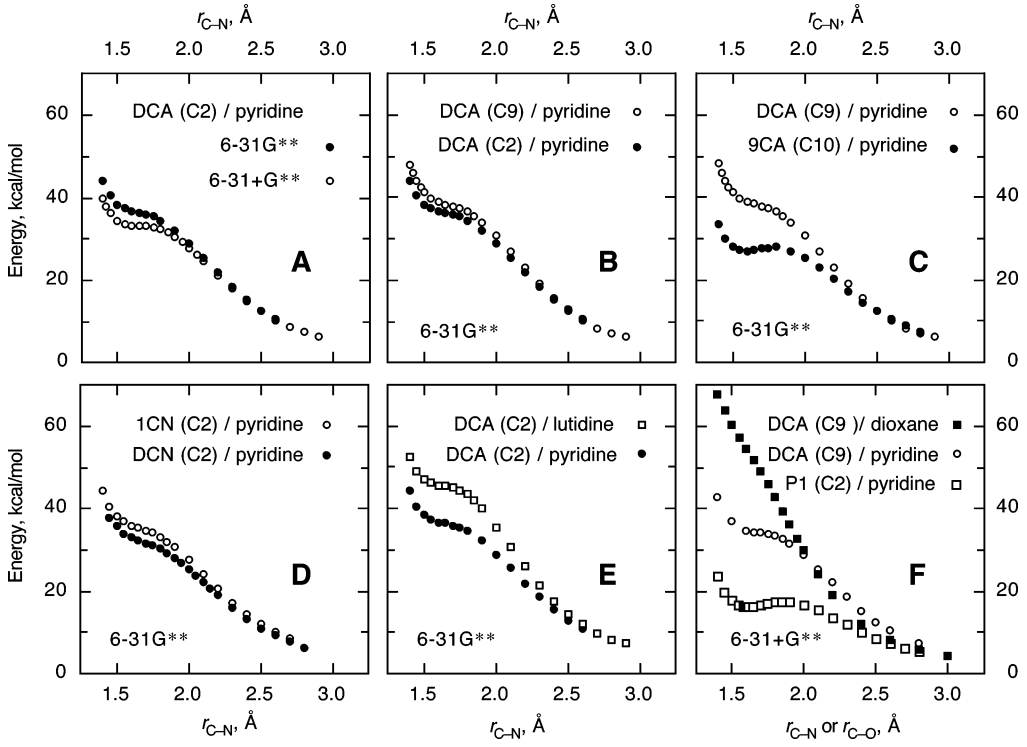

FIGURE 10. Computed energies as a function of separation distance, r_{C-N}, for ground state addition of pyridine at: (A) C2 of 9,10-dicyanoanthracene (DCA) using two different basis sets; (B) C2 and C9 of DCA; (C) C9 of DCA and C10 of 9-cyanoanthracene (9CA); (D) C2 of 1-cyanonaphthalene (1CN) and C2 of 1,4-dicyanonaphthalene (DCN); (E) C2 of DCA and addition of 2,6-lutidine to C2 of DCA; and (F) C2 of 2,4,6-triphenylpyrylium ion (P1). Figure 10F also compares the computed energies for addition of dioxane at C9 of DCA versus that of pyridine. The computations were performed using the B3LYP hybrid functional method, counterpoise corrected, in a dielectric continuum corresponding to acetonitrile, and with the basis sets indicated.

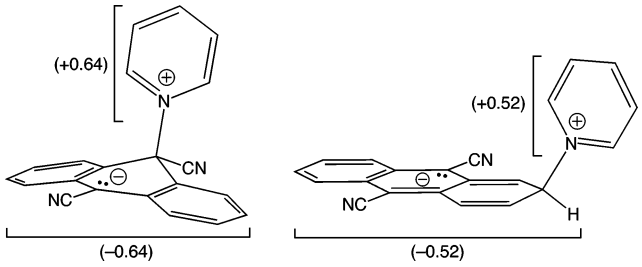

FIGURE 11. Computed structures and natural bond orbital (NBO) fragment charges for addition of pyridine to DCA at $r_{C-N} = 1.6$ Å.

In Figure 10B, the additions of pyridine to the C2 and C9 positions of DCA are compared. The structures and charge distributions near the inflection points at $r_{C-N} = 1.6$ Å are shown in Figure 11. The computed structures resemble resonance hybrids of ground and zwitterionic, bonded ET configurations, consistent with the bonded exciplex model proposed in Figure 9. The fractional charge transfer in the computed structures can be determined by summing the natural bond orbital (NBO) atomic charges on all of the atoms associated with the pyridine fragment. The fragment charges calculated this way show >50% charge transfer and are consistent with the ET configurations being slightly lower in energy than the ground configurations at $r_{C-N} = 1.6$ Å; that is, the curves for the ground and the bonded ET configurations in Figure 9 cross in both cases. The slightly larger extent of charge transfer for addition at C9 compared to that at C2 (64 vs 52%) is presumably because the ground-state curve rises in energy faster for C9 than C2 addition. As a consequence, curve crossing occurs at larger separation

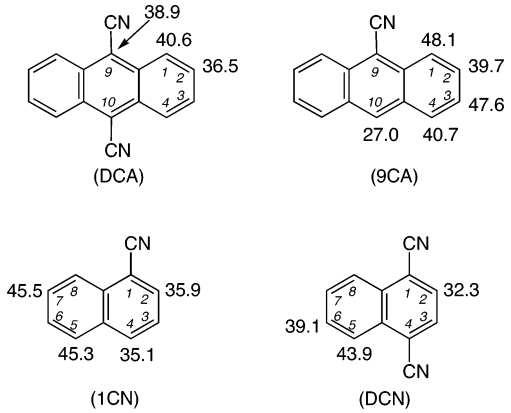

FIGURE 12. DFT-computed energies in kcal/mol (6-31G**, counterpoise-corrected in a dielectric continuum corresponding to acetonitrile) for reactions of 9CA, DCA, 1CN, and DCN with pyridine at different sites of the acceptors at C−N distance of 1.6 Å. Zero energy is defined by infinite separation of the reactants.

distances for addition to C9, resulting in greater bonded-state (zwitterionic) character.

The energies of the adducts formed by addition of pyridine to DCA at C1, C2, and C9 with $r_{C-N} = 1.6$ Å are compared in Figure 12. Addition at C1 and C2 results in slightly higher (1.7 kcal/mol) and lower (2.4 kcal/mol) energies, respectively, compared to addition at C9. Competing factors likely play a role in determining the stabilities of the various adducts. On the basis of the lower atom localization energy for the anionic fragment of the adduct,[26] addition at C9 is favored. This preference is apparently counterbalanced by the presence of the

cyano group at C9, which is destabilizing both sterically and electronically.[27] These competing factors for addition to DCA become reinforcing for addition to 9CA which, as shown in Figures 9C and 11, makes addition to C10 strongly preferred. For 9CA, the calculations additionally suggest that a shallow energy minimum (~1 kcal/mol) may exist on the ground-state surface.

Pyridine additions to 1-cyanonaphthalene (1CN) and 1,4-dicyanonaphthalene (DCN) have energy profiles similar to those calculated for DCA and 9CA (cf. Figure 10C,D). The computed energies for 1CN and DCN in the plateau region at $r_{C-N} = 1.6$ Å are summarized in Figure 12. In both cases, the energies for addition at the substituted ring are lower than those at the unsubstituted ring.

The energy profiles for all of the cyanoaromatic acceptors indicate that either no minimum or a very shallow energy minimum is present for the ground state of the pyridine adducts. This explains why no long-lived intermediate can be detected in the quenching reactions. Rapid nonradiative decay of the bonded exciplex leads to a ground state that is repulsive at the C−N bond distance of the exciplex, as shown schematically in Figure 9.

The calculations also explain the steric effect that hinders bond formation for the reactions with 2,6-lutidine (Figure 10E). The calculated energy in the plateau region of the ground state at 1.6 Å is 45 kcal/mol, ~10 kcal/mol higher than for the corresponding reaction of pyridine. The weaker bonding with lutidine decreases the rate constants for its reactions with the excited-state cyanoaromatic acceptors.

DFT computations were also performed for addition of pyridine to C2 of the cationic acceptor, triphenylpyrylium (P1, Figure 10F). As with the cyanoaromatic acceptors, significant deviation from repulsive behavior was observed, indicating a similar curve crossing between ground and bonded ET configurations. Similar to 9CA, the calculations indicate a shallow energy minimum (~1 kcal/mol) on the ground-state surface. As discussed above, the excited pyrylium sensitizers react with pyridine more slowly than the excited cyanoaromatic at equal driving force (Figure 5). This can be rationalized with the bonded exciplex model by recognizing that addition of pyridine to the pyrylium cations will result in steric destabilization due to the aryl group at C2, resulting in an overall weaker bonding interaction and thus a higher energy transition state leading to the bonded exciplex.

Finally, as discussed earlier, excited-state quenching by ethers is found to be less efficient than by pyridine (Figure 4). In fact, the rate constants for quenching by ethers are very similar to those of the conventional electron-transfer reactions of alkyl benzenes, suggesting that formation of bonded exciplexes is inefficient in these cases. DFT computations were performed for the addition of dioxane to DCA to understand this behavior. The energy profile as a function of the C9−O distance is shown in Figure 10F. In this case, deviation from purely repulsive behavior in the ground state is barely noticeable, indicating much weaker C−O bond formation compared to C−N bonding for pyridine. The weaker Lewis base character of the ethers compared to pyridine presumably results in a bonded ET configuration that is sufficiently high in energy that the rate constants for their formation cannot compete with those for conventional electron transfer.

2.4. Competing Quenching Mechanisms. The reactions of the cyanoaromatic excited states with 2,6-lutidine (Figure 6) exhibit quenching behavior that is consistent with competing formation of both bonded and conventional exciplexes. In the exothermic region for electron transfer, the rate constant data for reaction with ^{1}TCA* fit on the same curve as the conventional electron-transfer reactions. As electron transfer becomes increasingly endothermic, however, the rate constants for quenching by lutidine show increasingly positive deviations from the electron-transfer curve. In the exothermic region, the reaction presumably occurs by formation of a radical ion pair formation via conventional electron transfer. The larger than expected rate constants in the endothermic region, however, suggest formation of a bonded exciplex. This interpretation is supported by the DFT calculations (section 2.3) and the exciplex emission experiments. The observation of exciplex emission for DCN/lutidine in acetonitrile (Figure 7) demonstrates that conventional electron transfer at least partially occurs in this system. The fluorescence emission of the exciplex, however, is ca. 1/10 of the corresponding DCN/toluene exciplex, despite the fact that lutidine and toluene have similar oxidation potentials. This observation is consistent with the quenching rate constant. The quenching of ^{1}DCN* by lutidine via conventional electron transfer ($\Delta G = 0.07$ eV) is predicted from curve 1 in Figure 6 and the driving force for electron transfer to have a rate constant of 8.5×10^8 M^{-1} s^{-1}. This is ~15% of the experimental quenching rate constant, 5.6×10^9 M^{-1} s^{-1}. Thus, *both* the exciplex intensity and the quenching rate constant indicate that ~85−90% of the quenching reaction proceeds via bonded exciplex formation and the remainder by conventional electron transfer.

3. Concluding Remarks

The important conclusion from this work is that the rate constants for charge-transfer quenching of excited electron acceptors by pyridine cannot be explained in terms of conventional exciplex/radical ion pair intermediates. Instead, the experimental data are best rationalized by formation of a previously undescribed bonded exciplex intermediate. This conclusion is supported by DFT computations that clearly indicate the presence of a low-energy charge-transfer-bonded configuration that mixes with the neutral reactants.

For the pyridine quenching reactions, a bonded exciplex intermediate can be inferred from analysis of the bimolecular reaction kinetics because formation of the conventional intermediates is thermodynamically unfeasible. In other excited-state quenching reactions, where formation of conventional exciplex/radical ion pair intermediates is thermodynamically favorable, formation of a bonded exciplex may still occur. An initially formed conventional exciplex/radical ion pair can subsequently lead to a bonded exciplex because this follow-up step could be considerably exothermic. In these cases, however, sequential formation of such a bonded exciplex would not be detectable from the quenching kinetics because the quenching and bonded exciplex formation steps are kinetically uncoupled. Evidence for formation of a bonded exciplex under these conditions may nonetheless be obtained from studies of the kinetics of *deactivation* of the intermediates, specifically by unusually high rate constants for nonradiative decay. Preliminary investigations on the rate constants for radiationless decay in the charge-transfer

(26) Brown, R. D. *Quart. Rev. (London)* **1952**, *6*, 63.

(27) For comparison, the C−N bond dissociation energies of the *N*-methylpyridinium and *N*-cyanomethylpyridinium cations calculated at the B3LYP/6-31G* level of theory are 111 and 84 kcal/mol, respectively.

quenching reactions of alkoxybenzenes compared to alkylbenzenes as donors suggest that deactivation via a bonded exciplex may be involved in the former reactions.[28]

Other possible examples of bonded exciplex formation include photochemical cycloaddition reactions that occur via emitting exciplex intermediates.[29] We now recognize that these, and a large number of other reactions that involve bond-making and bond-breaking steps,[7] may involve bonded exciplex intermediates. Thus, the importance of a bonding contributor to the general description of exciplexes may extend well beyond the reactions described here. Further mechanistic investigation of these possibilities are in progress in our laboratories, together with a quantitative analysis of the three-state mixing model for bonded exciplex formation and decay.

Experimental Section

The cyanoaromatic acceptors and alkylbenzene donors were available from previous studies. Pyridine and 2,6-lutidine were freshly distilled before use. All solvents were HPLC grade and were used as received. The pyrylium salts and the cyanoaromatics were gifts from the Eastman Kodak Company. The methods and apparatus for steady-state emission and absorption spectroscopy, for steady-state photolysis, for nanosecond, picosecond, and femtosecond transient absorption spectroscopy, and for lifetime measurements by single photon counting have all been previously described.[11e,16a] Where appropriate, the picosecond transient spectra were corrected for chirp in the analyzing pulse; see the Supporting Information for an example.[30]

All calculations were performed using Jaguar[23] v6.5 (build 112) on a Pentium III Xeon 1.7 GHz Linux desktop machine or 2.2 GHz dual-core Opteron 275 running CentOS 4.2 or 2.8 GHz Xeon running CentOS 4.3. Typical CPU time on the 2.2 GHz machine for B3LYP-DFT/6-31G** optimizations were under 3 h and 5−10 h for B3LYP-DFT/6-31+G** optimization. Default settings were used throughout, except that the convergence criteria energy change was set to 10^{-6} Hartree. The solvent, acetonitrile, was defined in Jaguar using the following parameters: dielectric constant = 35.0, MW = 41.05, and density = 0.786.

In order to ensure that the global minimum was identified, torsion scans at fixed distances about the r_{C-N} or r_{C-O} bond using a 10° increment were performed for representative systems. The magnitude of the counterpoise correction at 1.6 and 2.8 Å is ∼5.4 and 2.6 kcal/mol for 6-31G**, respectively, and ∼1.4 and 0.4 kcal/mol for the same distances using 6-31+G**.

The fraction of charge transfer (f_{CT}) was calculated from the atomic charges of the two moieties calculated using the NBO[31] option in Jaguar.

Acknowledgment. Research support was provided by the National Science Foundation (CHE-9812719) and the Research Corporation. We thank Sason Shaik (Hebrew University) for stimulating discussions regarding the valence bond configuration mixing model. We are grateful to Ralph Young of the Eastman Kodak Company for numerous discussions, and to Jerome Lenhard and Marcel Madaras of the Eastman Kodak Company for the electrochemical potentials of the cyanoaromatics and the pyrylium salts.

Supporting Information Available: Chirp correction for the spectrum of the excited DCA in pyridine, transient absorption spectra of excited DCA in different solvents, spectra of excited DCA in pyridine as a function of time, spectra of excited DCA in benzene in the presence of pyridine as a function of time, and spectra of excited DCA in acetonitrile in the presence of pyridine as a function of time. Also available is the quenching rate constant and reaction free energy data for reaction of excited DCA with alkylbenzenes for Figures 5 and 6, and data showing the relationship between oxidation and ionization potential for alkylbenzenes. This material is available free of charge via the Internet at http://pubs.acs.org.

JO071157D

(28) Fleming, C. N.; Dinnocenzo, J. P.; Gould, I. R.; Farid, S. Unpublished results.

(29) (a) Mattes, S. L.; Farid, S. *Acc. Chem. Res.* **1982**, *15*, 80. (b) Williams, J. L. R.; Farid, S.; Doty, J. C.; Daly, R. C.; Specht, D. P.; Searle, R.; Borden, D. G.; Chang, H. J.; Martic, P. A. *Pure Appl. Chem.* **1977**, *49*, 523. (c) Caldwell, R. A.; Ghali, N. I.; Chien, C.-K.; DeMarco, D.; Smith, L. *J. Am. Chem. Soc.* **1978**, *100*, 2857. (d) Mizuno, K.; Pac, C.; Sakurai, H. *J. Am. Chem. Soc.* **1974**, *96*, 2993.

(30) Fleming, G. *Chemical Applications of Ultrafast Spectroscopy. International Series of Monographs on Chemistry 13*; Oxford University Press: New York, 1986.

(31) Glendening, E. D.; Badenhoop, J. K.; Reed, A. E.; Carpenter, J. E.; Bohmann, J. A.; Morales, C. M.; Weinhold, F. *NBO 5.0*; Theoretical Chemistry Institute, University of Wisconsin: Madison, WI, 2001.